ENVIRONMENTAL RESEARCH LETTERS



**LETTER • OPEN ACCESS**

# Integrated assessment of the net carbon footprint of small hydropower plants

To cite this article: Lluís Gómez-Gener *et al* 2023 *Environ. Res. Lett.* **18** 084015

ENVIRONMENTAL RESEARCH
LETTERS



OPEN ACCESS

RECEIVED
26 October 2022

REVISED
16 May 2023

ACCEPTED FOR PUBLICATION
20 June 2023

PUBLISHED
24 July 2023



LETTER

# Integrated assessment of the net carbon footprint of small hydropower plants

**Lluís Gómez-Gener**[1,2,3,*], **Marina Gubau**[1], **Daniel von Schiller**[1,4], **Rafael Marcé**[5,6] **and Biel Obrador**[1,2]

[1] Departament de Biologia Evolutiva, Ecologia i Ciències Ambientals, Facultat de Biologia, Universitat de Barcelona (UB), Av. Diagonal 643, Barcelona, Spain
[2] Institut de Recerca de la Biodiversitat (IRBio), Universitat de Barcelona (UB), Barcelona, Spain
[3] Centre for Research on Ecology and Forestry Applications, Universitat Autònoma de Barcelona, Campus de Bellaterra, Edifici C, Cerdanyola del Vallès, Barcelona, Spain
[4] Institut de Recerca de l'Aigua (IdRA), Universitat de Barcelona (UB), Barcelona, Spain
[5] Catalan Institute for Water Research (ICRA), Girona, Spain
[6] University of Girona, Girona, Spain
[*] Author to whom any correspondence should be addressed.

**E-mail:** gomez.gener87@gmail.com

**Keywords:** footprint, life cycle, carbon, emission, reservoir, impoundment, hydropower

Supplementary material for this article is available online

## Abstract

Global assessments evaluating greenhouse gas emissions and climate benefits of hydropower rely on life cycle assessments (LCAs). However, small hydropower plants (i.e. installations with less than 10 MW; SHPs), are largely underrepresented in such schemes, despite their widespread proliferation and well-known ecological concerns. Here we quantified, partitioned, and compared the net carbon (C) footprint of four temperate SHPs with different operation designs over a 100 year time horizon. In contrast with previous hydropower LCAs studies, we followed an integrative net C footprint approach accounting for all potential sources and sinks of C within the life cycle of the studied SHPs, including both biogenic and non-biogenic sources, as well as for the pre- and post-impoundment stages involved in the flooding of the reservoir. We found that the areal and system-level C emissions were mostly driven by the residence time of the impounded water, which in turn was linked to the SHP operation type. The power installed in the SHPs did not have a relevant role on the net C fluxes. Accordingly, SHPs with smaller water storage capacity were almost neutral in terms of the C footprint. In contrast, SHPs with water storage facilities prolonged the water residence time in the reservoir and either acted as a source or sink of C. The long water residence time in these SHPs promoted either emission of biogenic gases from the surface or C storage in the sediments. Our work shows that integrative net C footprint assessments accounting for different operation designs are necessary to improve our understanding of the environmental effects of SHPs.

## 1. Introduction

In the current context of Climate Change, any industrial activity faces the challenge of aligning its economic and technical competitiveness with the environmental sustainability of its activities (Kumar *et al* 2011). Hydropower, despite being often presented as a green energy in terms of carbon footprint (CF), is not an exception. As any energy supply system, the construction and operation of hydropower plants (HPs) involves the production and emission of greenhouse gases (GHGs) that may contribute to climate change (Weisser 2007, Kumar *et al* 2011, Raadal *et al* 2011). Existing evidence suggests that biogenic carbon (C) emissions (i.e. carbon dioxide ($CO_2$) and methane ($CH_4$) originated through biogeochemical processes and released to the atmosphere) from HP reservoirs are far higher and more geographically widespread than previously assumed (Deemer *et al* 2016, Rosentreter *et al* 2021). Yet, reported C emissions and associated CFs estimates remain uncertain, varying more than four-fold in recent analyses (Hertwich

2013, Scherer and Pfister 2016, Bertassoli et al 2021). The main reasons for this variability are: (i) the large uncertainty associated with the use of multiple approaches to assess hydropower CFs (Kumar et al 2011, Raadal et al 2011); (ii) the lack of more suitable (and standardized) definitions for size categories and limited consideration of potential descriptors of environmental impacts (e.g. dam height, reservoir area, water residence time, and operating procedures) (Couto and Olden 2018); and (iii) the large underrepresentation of small HPs (SHPs) within climate impact assessments. Altogether, these limitations hinder a comprehensive assessment of the actual and future climate impact (or CF) of hydropower across climates, pre-impoundment land cover types, and HP sizes and technologies.

In recent years, global assessments evaluating GHG emissions and climate benefits of hydropower have increasingly relied on life cycle assessments (LCAs; Varun et al 2009). LCAs are an environmental evaluation of all the stages involved in creating a product over a certain period (typically its life cycle), and is usually expressed as C emissions (in g $CO_2$ equivalents, $CO_2$e) per energy generated (kWh). For hydropower, the LCA consists of three main stages. The first one is the pre-impoundment stage, which accounts for all C that would have been emitted or stored if the river system had remained in its natural state. This includes the C fluxes associated to the original terrestrial ecosystem and the fluvial ecosystem (stream or river C exchange). The second one is the post impoundment stage, which includes: (i) the C fluxes associated to the construction, operation and maintenance activities (hereafter, non-biogenic post-impoundment C fluxes), (ii) the C emissions generated by the decomposition of biomass in flooded land (Deemer et al 2016), (iii) the C emissions associated to turbine passage of water (Guérin et al 2006), and (iv) the flux of C stored in reservoir sediments (Mendonca et al 2016) (hereafter post-impoundment biogenic C fluxes). Because the global warming potential of $CH_4$ is 30-fold higher compared to that of $CO_2$ over a 100 year time horizon, its emission to the atmosphere are of major concern from a climate perspective (Friedlingstein et al 2019, Soued et al 2022). $CH_4$ emissions exhibit an extreme intra-reservoir spatial patchiness (Maeck et al 2013, Beaulieu et al 2016) and unpredictable timing (McGinnis et al 2006), which make an accurate quantification of ecosystem $CH_4$ fluxes difficult. Moreover, the so-called drawdown areas of reservoirs, where sediment is exposed to the atmosphere due to water-level fluctuations, have been pointed out as a widespread significant source of $CO_2$ (Marcé et al 2019, Almeida et al 2019a, Keller et al 2021) and a potential source of $CH_4$ (Yang et al 2014, Serça et al 2016, Paranaíba et al 2022). The third and last stage is the decommissioning, which includes the C fluxes associated to the dismantling of the infrastructure (Pacca 2007).

To facilitate the comparison of hydropower CFs with broader electricity generation technologies (Edenhofer et al 2011), most LCAs of hydropower GHG emissions have been exclusively based on 'non-biogenic' C fluxes derived from the construction, operation and maintenance stages (Varun et al 2012, Turconi et al 2013). However, current evidence suggests that non-biogenic fluxes often play a minor role compared to those associated with the decomposition of flooded vegetation and soil organic matter (Barros et al 2011, Soued et al 2022). This is especially relevant in HPs with large storage facilities and long residence time, and has brought to unexpectedly large variability in most recent hydropower CFs estimates (Scherer and Pfister 2016). In addition, current LCA models are based on 'gross' estimates that typically do not account for pre-impoundment C fluxes and organic C sedimentation and burial. In those cases, the LCA outcome is incomplete because it neglects critical aspects, such as how large C emissions would have been in the absence of the reservoir, or how much they may have been displaced elsewhere and what is the temporal evolution of the post-impoundment emissions (Prairie et al 2018). Therefore, the application of LCAs integrating all the potential fluxes (i.e. pre- and post- impoundment and biogenic and non-biogenic) is a first key step to reduce the uncertainty of hydropower CFs (Bertassoli et al 2021, Prairie et al 2021).

The size of a given HP is commonly defined based on its potential power generation capacity (or installed power capacity, in $W$), which is the maximum capacity of hydropower production assuming optimal hydrologic conditions and turbine efficiency (Couto and Olden 2018). About 70% of countries with formal definitions classify SHPs as installations with less than 10 MW (Kelly-Richards et al 2017, Couto and Olden 2018), which is increasingly recognized as the international standard (WSHPDR 2019). On the other hand, large HPs (LHPs) are classified as HPs with an installed power capacity larger than 10 MW. Despite covering <5% of the global reservoir surface area (Downing et al 2006, Lehner et al 2011) and contributing to only 11% of the global electricity generation, SHPs represent 91% of the total number of HPs currently operating or under construction (Couto and Olden 2018; figure 1(a)). Furthermore, political and economic incentives for renewable energy development, in part grounded on the perception that 'smaller' equates to lower socioecological impact (Couto and Olden 2018), have contributed to a global 'boom' of SHPs construction (Zarfl et al 2015, Belletti et al 2020, Zarfl and Lehner 2020). Although SHPs are spreading around the world at a faster pace than LHPs (on average, 11 SHPs for every LHP), distinct geographic patterns of SHP construction are apparent, reflecting differences in socioeconomic conditions, varying regulations, and contrasting hydrologic potential (Couto and Olden 2018).

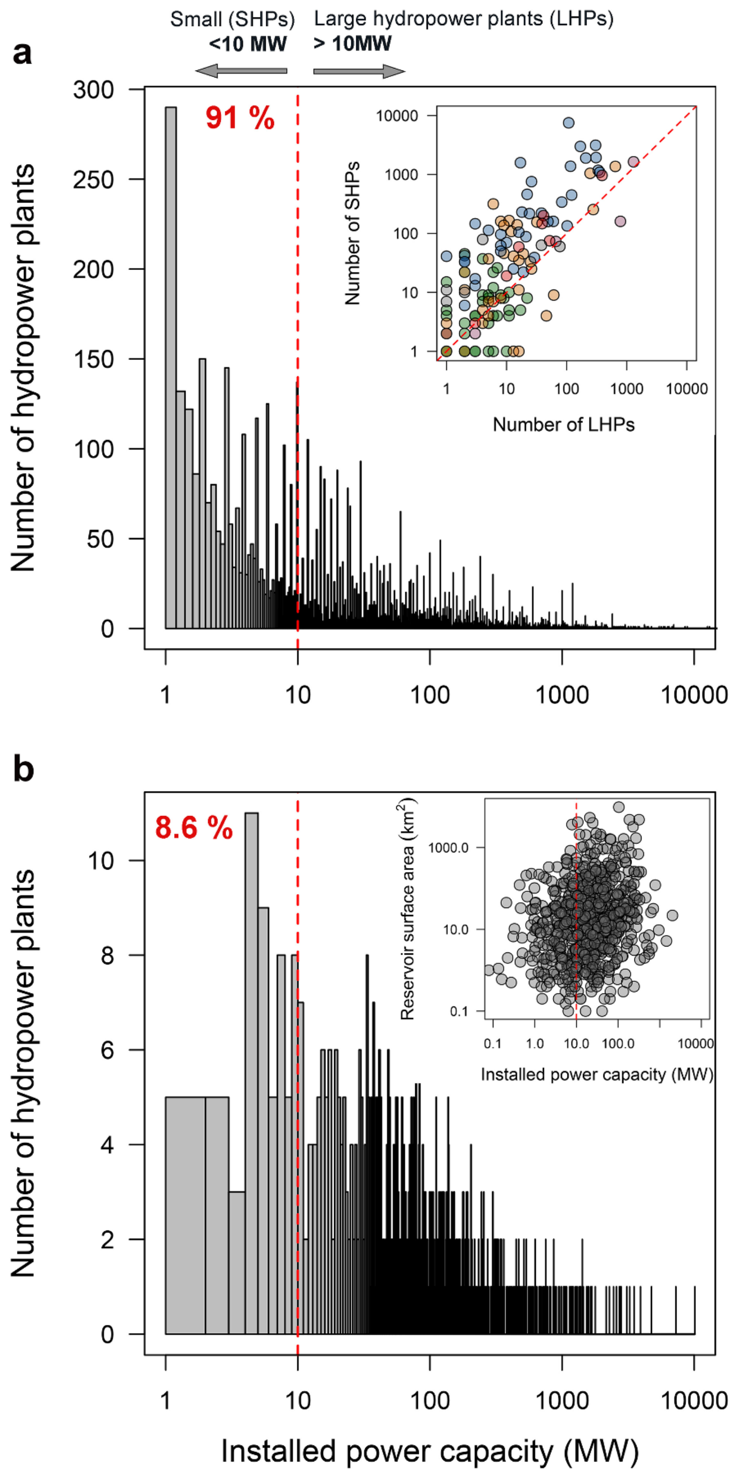


**Figure 1.** (a) Histogram showing the frequency distribution of global hydropower plants (HPs) by generation capacity ($n = 90\,231$; data from Couto and Olden 2018). SHPs represents 82 891 (91%) of global HPs. Inset shows the relationship between the number of LHPs and SHPs in 203 countries worldwide, color coded by continent (blue = Europe, $n = 42$; orange = Asia, $n = 49$, red = America, $n = 33$; green = Africa, $n = 54$; grey = Oceania, $n = 24$). (b) Histogram showing the frequency distribution of HPs by generation capacity, only when carbon footprint (CF) data through LCAs of biogenic carbon gas emissions is available ($n = 1467$; data from Scherer and Pfister 2016). Only 64 (8.6%) of available CF data corresponds to SHPs. Inset shows that for the same data set, HPs generation capacity is unrelated to reservoir storage capability (measured as reservoir water surface area). The red dashed line represents the most recognized criterion to differentiate SHP from large HP (10 MW, Couto *et al* 2018, Lange *et al* 2018).

The proliferation of SHPs is of increasing concern because of the physical and ecological consequences of river network impoundment and fragmentation at different scales (Kibler and Tullos 2013, Anderson *et al* 2015, Lange *et al* 2018). Although the ecological impacts of SHP are highly variable, the cumulative effects of cascading plants (i.e. multiple and consecutive HPs within a river section or the river network) are likely to be greater than the sum of the impacts from each individual plant (Lange *et al* 2018). Small impoundments have recently been found to also alter the biogeochemical processes that control the production and emission of C in river networks by increasing the residence time of water and organic matter (Maeck *et al* 2013, Gómez-Gener *et al* 2018, Maavara *et al* 2020). Consequently, the CF of SHPs is in most cases disproportionally higher than that of LHPs (Räsänen *et al* 2018, Almeida *et al* 2019b). Unfortunately, the proliferation of SHP infrastructures is not aligned with a similar effort on quantifying their CFs. Only 8.6% out of the assessments of hydropower CFs ($n$ = 1567) have been carried out in SHPs (figure 1(b)). Moreover, facilities designated as SHPs have substantially different hydrodynamics (e.g. water residence time, storage capacity, or surface area; figure 1(b)) as they host a diversity of operation modes (e.g. storage and non-storage, diversion and non-diversion). Storage SHPs typically have large hydraulic head and storage volume, long water residence times, and control over the rate at which water is released from the impoundment. Conversely, non-storage (or run-of-river) SHPs, the most common and often overlooked type of SHP, have small storage volume and short residence time (Poff and Hart 2002). Reservoir hydrology might potentially be a good predictor of the CF in SHPs, as water residence time is a key variable affecting the biophysical regime of rivers (Poff and Hart 2002, Catalán *et al* 2016, Palmer and Ruhi 2019). However, this potential linkage has not been yet resolved, thus limiting our ability to fully understand the environmental benefits of small hydropower (compared with other type of energies) and, in turn, be in a stronger position to guide the future of hydropower in a changing climate.

The aim of this paper is to quantify and partition the net CF of SHPs, with special emphasis on the differences among operation types and on the role of gross vs net quantifications. To do this, we carried out an integrated LCA on four SHPSs over a time span of 100 years. The LCAs accounted for all potential sources and sinks of C in the studied SHPs (both from biogenic and non-biogenic origin) as well as for the pre- and post-impoundment stages involved in the flooding of a reservoir.

## 2. Methods

### 2.1. Study sites

We estimated the CF of four SHPs corresponding to two operation types: two non-storage (i.e. run-of-river) and two storage, all located in the North of the Iberian Peninsula (table 1; figure S1). We selected these study sites from a detailed inventory of hydroelectric power plants of the Basque, Spain Country (EVE 1995; IKAUR-EKOLUR 2006; PHDHCO 2013). All sites were located within a relatively small geographical area in order to minimize heterogeneity in climatic, land use, and geochemical conditions.

### 2.2. Integrated LCA

To quantify the CF (in g $CO_2$e kWh$^{-1}$) of the four SHPs, we applied a LCA over a time horizon of 100 years (figure 2, table S1). The LCA includes (i) the net C flux associated with the SHPs over the reference life-cycle period (in g $CO_2$e 100 yr$^{-1}$), and (ii) the total energy produced by the SHPs over the same time horizon (in kWh 100 yr$^{-1}$):

$$\mathrm{CF}_{100} = \frac{\text{Net C flux}_{100}}{\text{Total energy production}_{100}} \quad (1)$$

We obtained the Total energy production$_{100}$ from the annual energy production (in kWh yr$^{-1}$) over 100 years. We derived the annual energy production from the installed power capacity data at each plant (in MW, see table 1) and the daily hours of turbine activity (h d$^{-1}$). Based on real daily production statistics provided by the hydropower companies, we set a constant value of 10 h d$^{-1}$ of turbine activity over the entire study period. This value is consistent with daily production values from other SHPs (Zhang *et al* 2007, Varun *et al* 2012, Pang *et al* 2015). We obtained the Net C flux$_{100}$ by subtracting the C flux associated with the dam construction and subsequent flooding over 100 years (Post - impoundment C flux$_{100}$; in g $CO_2$e 100 yr$^{-1}$) from the potential C flux in the same study area if not flooded (Pre - impoundment C flux$_{100}$; in g $CO_2$e 100 yr$^{-1}$) over the same time horizon:

$$\text{Net C flux}_{100} = \text{Post - impoundment C flux}_{100} - \text{Pre - impoundment C flux}_{100}. \quad (2)$$

**Table 1.** Design operational and morphometrical characteristics of the four SHPs.

| | Operational characteristics | | | | | Morphometrical characteristics | | |
|---|---|---|---|---|---|---|---|---|
| SHP | Operation type | Installed power capacity (MW) | Annual power production (GWh yr$^{-1}$) | Power density (MW km$^{-2}$) | Extraction depth (m) | Total storage capacity (hm$^3$) | Total surface area (km$^2$) | Dam height (m) |
| 1 | Non-storage SHP | 0.3 | 1.10 | 57.7 | 0 (surface) | 0.007 | 0.005 | 2.0 |
| 2 | Non-storage SHP | 0.3 | 1.10 | 49.18 | 0 (surface) | 0.012 | 0.006 | 2.3 |
| 3 | Storage SHP | 1.3 | 4.54 | 0.6 | 25 | 43.7 | 2.0 | 79.5 |
| 4 | Storage SHP | 2.5 | 9.37 | 16.45 | 15 | 1.9 | 0.2 | 36.0 |

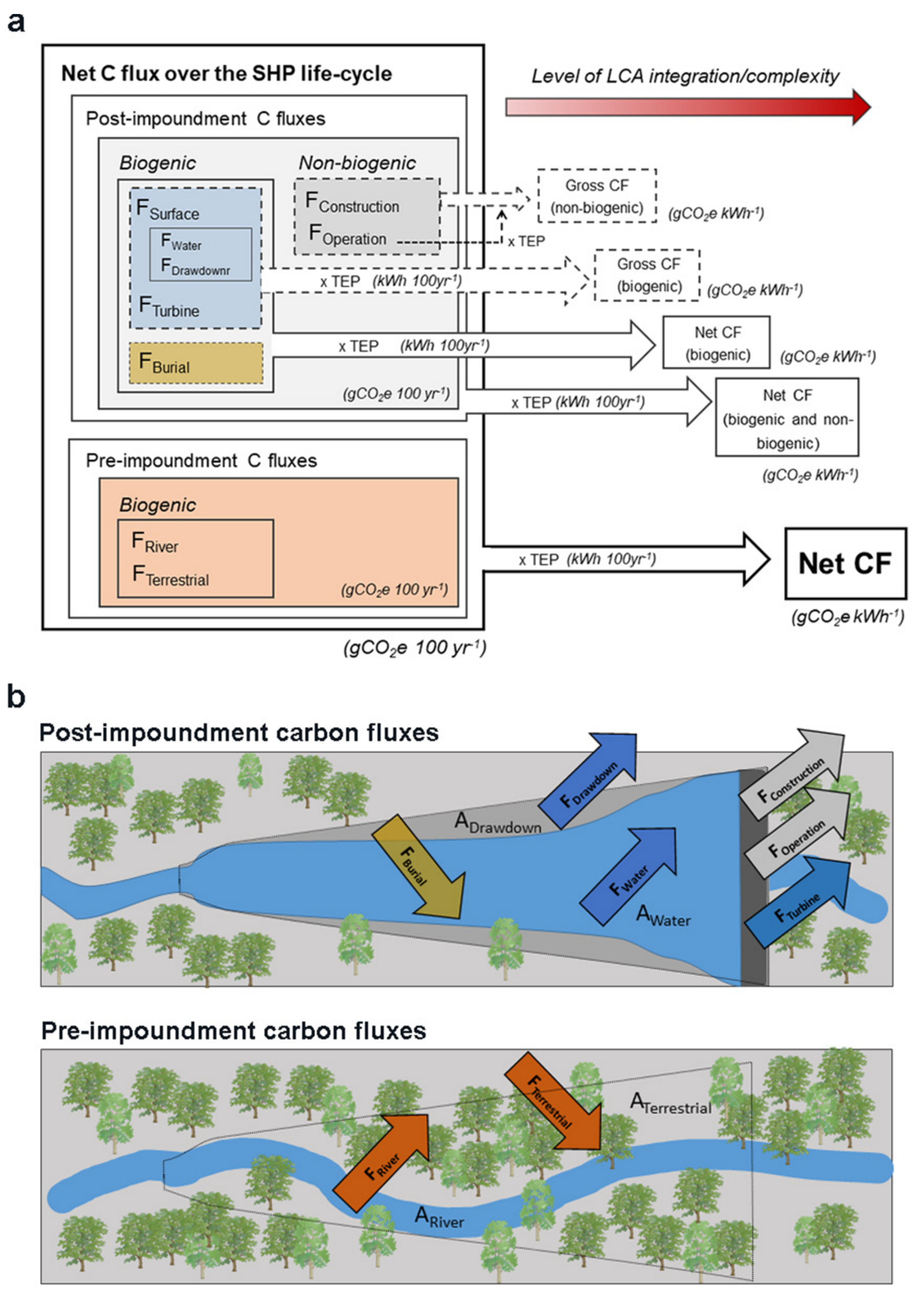


**Figure 2.** (a) Diagram with flux components considered in the integrated life-cycle analysis (LCA) to assess the 'net' carbon footprint (CF) of hydropower plants. Dashed and solid line box contour represent fluxes and pathways classically considered to respectively assess the 'gross' and 'net' carbon footprint of hydropower plants (sorted by level of complexity or integration of the model). (b) Scheme of the pre- and post-impoundment carbon flux components and surface areas considered in the LCA model. Dashed line represents the post-impoundment reservoir surface. Note that fluxes that represent a source from the system to the atmosphere are shown with an arrow pointing up, while fluxes representing sinks are shown with an arrow pointing down. Note that the carbon flux between the reservoir surface and the atmosphere accounts for both the flux from the surface water ($F_{\text{Water}}$) and the flux from the surface of the emerged sediment ($F_{\text{Drawdown}}$). See table S1 for detailed descriptions and calculations of the LCA flux components. The total energy or power production (TEP) refers to the total estimated electrical production by each SHP over its life-cycle period (i.e. 100 years).

The post-impoundment C flux$_{100}$ includes (i) the net C balance associated with the flooding of rivers and forests (Post - impoundment biogenic C flux$_{100}$, in g $CO_2$e 100 yr$^{-1}$), and (ii) the net C flux associated with the construction and operation of the SHPs (Post - impoundment non - biogenic C flux$_{100}$, in g $CO_2$e 100 yr$^{-1}$). We assessed these fluxes over a time horizon of 100 years:

$$\text{Post - impoundment biogenic C flux}_{100} = F_{\text{Surface}} + F_{\text{Turbine}} - F_{\text{Burial}} \quad (3)$$

$$\text{Post - impoundment non - biogenic C flux}_{100} = F_{\text{Construction}} + F_{\text{Operation}} \quad (4)$$

$$\text{Post - impoundment C flux}_{100} = (F_{\text{Surface}} + F_{\text{Turbine}} - F_{\text{Burial}}) + (F_{\text{Construction}} + F_{\text{Operation}}) \quad (5)$$

where $F_{surface}$ is the flux from the reservoir surface area, $F_{turbine}$ is the turbine water passage, $F_{Burial}$ is the long-term C accumulation in sediments, $F_{construction}$ is the flux associated with the construction of the plant, and $F_{operation}$ is the flux associated with its regular operation and maintenance.

The pre-impoundment C flux$_{100}$ in equation (2) includes the net balance of potential C fluxes in the same reservoir area assuming it was not flooded because of the dam construction, estimated over the same time horizon of 100 years (figure 2):

$$\text{Pre - impoundment C flux}_{100} = F_{\text{River}} + F_{\text{Terrestrial}} \quad (6)$$

where $F_{River}$ and $F_{Terrestrial}$ are, respectively, the fluxes from the river and terrestrial ecosystems surfaces before the impoundment of the river.

### 2.3. LCA flux components

*2.3.1. Post-impoundment biogenic fluxes*

We determined the post-impoundment biogenic C fluxes (except $F_{Burial}$, see below) by sampling under two contrasted hydrological conditions: winter (January 2016 campaign) and summer (June 2016 campaign). We obtained annual C fluxes by averaging values from these two sampling campaigns.

We estimated the C fluxes from the reservoir surface area, including both the water surface and the drawdown areas by multiplying the daily areal emission rates of each flux (in $gCO_2e\ m^{-2}\ d^{-1}$) by the area occupied by each flux component (see extended methodology in table S1). Large systems show high spatial variability in C gas emission rates (Beaulieu *et al* 2016). Therefore, in the two larger systems studied (SHP 3 and SHP 4), we established different sampling zones (i.e. tail, center, and dam) based on depth profiles. We obtained the area of each zone by combining field depth profiles and aerial imagery (table S3). For each SHP and date, we estimated the C flux associated with the turbine water passage ($F_{Turbine}$) from the volume of water turbinated by the concentration gradient between the reference water (upstream river reach) and the reservoir water near the turbine inflow ($\Delta C_i$, table S1). Finally, the C flux associated with the long-term sedimentation of C in the reservoir bottom ($F_{Burial}$) was obtained from the sedimentation rates for each system and the measured organic carbon content in the sediment (see extended methodology in table S1).

*2.3.2. Post-impoundment non-biogenic fluxes*

We derived (not measured) the post-impoundment C fluxes associated with the construction and operation of the power plants from the functions reported in Varun *et al* (2012), which allow to scale these emissions to the type of plant, the hydraulic head, and the installed power (see table S2). We extrapolated the fluxes obtained for each SHP to 100 years, which is the time horizon set for all the fluxes and studied SHPs (see extended methodology in table S1).

*2.3.3. Pre-impoundment fluxes*

We determined the biogenic gaseous C fluxes ($CO_2$ and $CH_4$) associated with the exchange between the atmosphere and the surface of existing ecosystems (rivers and forests) before the river impoundment by multiplying the current C fluxes of the upstream riverine and terrestrial ecosystems and their relative areas (see extended methodology in table S1).

## 3. Results

### 3.1. Areal C fluxes

The mean areal post-impoundment biogenic C flux of the four studied SHPs was 34.2 g $CO_2e\ m^{-2}\ d^{-1}$ (range = −12.9–134.4 g $CO_2e\ m^{-2}\ d^{-1}$; figure 3(a)). The magnitude and the relative contribution of the different flux components to the total areal C fluxes (turbine vs. surface vs. burial) was largely determined by the impounded water surface area and the operation type of each SHP (i.e. non-storage vs. storage SHPs, table 1). The two SHPs operating without storage reservoirs (SHP 1 and SHP 2; table 1) showed relatively low but positive areal C fluxes (i.e. acted as a source of C to the atmosphere), with a major contribution from the turbine component (74% and 93% of the areal C fluxes, respectively). The two SHPs operating with storage reservoirs (SHP 3 and SHP 4; table 1) showed higher but opposed potential for either storage of C in the sediment (down to −31.8 g $CO_2e\ m^{-2}\ d^{-1}$ in SHP 3) or evasion of C gases from the SHP surface (up to 130.3 g $CO_2e\ m^{-2}\ d^{-1}$ in SHP 4).

The areal C efflux from the surface of the two SHPs with storage facilities (water and drawdown zones) was dominated by $CH_4$ (average between SHP 3 and SHP 4 = 71.4 g $CO_2e\ m^{-2}\ d^{-1}$; figure 3(b)). In contrast, the $CO_2$ emission flux was of minor importance in the larger systems (mean for SHP 3 and SHP 4 = 5.5 g $CO_2e\ m^{-2}\ d^{-1}$; figure 3(b)). Among the potential pathways for $CH_4$ evasion, the diffusive $CH_4$ efflux contributed 74% of the total C evaded from the surface of SHP 3, while $CH_4$ ebullition made up 67% of the total C evaded from SHP 4 (figure 3(b)). Finally, the C emitted from emerged sediments was only significant in SHP 3, accounting for up to 11% of the total 18.8 g $CO_2e\ m^{-2}\ d^{-1}$ emission flux by the SHP (figure 3(b)). In contrast, the evasion rates from the water surface of SHP 4 (130.0 g $CO_2e\ m^{-2}\ d^{-1}$) were considerably higher than those from the drawdown area (4.98 g $CO_2e\ m^{-2}\ d^{-1}$; figure 3(b)).

Contrarily to the post-, the mean areal pre-impoundment C fluxes from biogenic origin (i.e. areal river and terrestrial flux; g $CO_2e\ m^{-2}\ d^{-1}$), were relatively low (always below 7.34 g $CO_2e\ m^{-2}\ d^{-1}$) and showed low variability across SHPs and operation types (figure 3(c)).

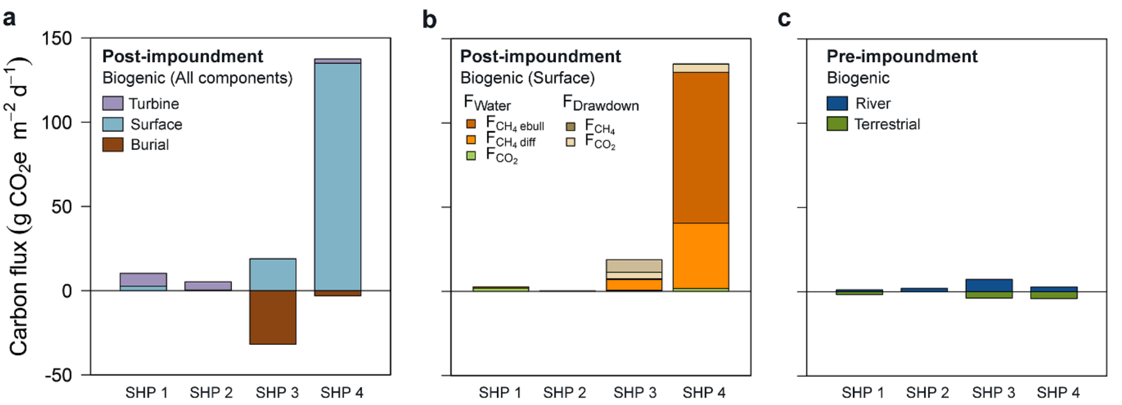


**Figure 3.** (a) Mean daily post-impoundment biogenic carbon areal fluxes of the four SHPs (b) mean daily post-impoundment biogenic carbon areal fluxes of the four SHPs broken up by surface components: water ($F_{Water}$) and drawdown ($F_{Drawdown}$); and carbon gas emission pathway: $CO_2$ (only diffusion) and $CH_4$ (either diffusion or ebullition). (c) Mean daily pre-impoundment biogenic carbon areal fluxes of the four SHPs. Positive carbon fluxes represent carbon gas release from the reservoir to the atmosphere (i.e. the flux component acts as a source of $CO_2$ or $CH_4$), whereas negative fluxes indicate carbon gas uptake in the reservoir (i.e. the flux component acts as a sink of $CO_2$ or $CH_4$). Note that the SHPs are sorted by installed power capacity (see table 1).

Consequently, the areal C flux balance between them (considering the opposite direction of the two pre-impoundment flux components) remained close to zero in all the studied SHPs regardless of the size of the system and its operation type (from −1.30 to 3.62 g $CO_2$e $m^{-2}$ $d^{-1}$; figure 3(c)).

### 3.2. System-level C fluxes

The differences in C fluxes between the two types of SHPs for both post- and the pre-impoundment conditions were notorious when the surface area of each system was considered, i.e. when addressing system-level C fluxes (in Gg $CO_2$e $yr^{-1}$; figure S3 and table S4). Both the net post- and pre-impoundment system C fluxes at the annual scale were, in absolute terms, three orders of magnitude lower in the non-storage SHPs compared with the storage SHPs. Similarly, the relative contribution of different C flux components to the net SHP system balance differed between the two operation types. In the two non-storage SHPs, the non-biogenic C fluxes ($F_{Construction}$ and $F_{Maintenance}$) and the C flux associated with the turbine water passage ($F_{Turbine}$) were the most significant C sources contributing, on average, 82.7% of the total annual C emitted (table S4). In contrast, in the two storage SHPs the non-biogenic fluxes were of minor importance in comparison with the biogenic C fluxes. The flux from the surface of the impoundment (for SHP 4) and burial flux (for SHP 3) dominated the post-impoundment SHP share (96.3% in SHP 4, and 89.6% in SHP 3). Finally, the rest of the C flux components were less influential and similarly important for the total annual C emission budget (table S4). Results of the error propagation for the system fluxes for each SHP in table S5.

### 3.3. Net CF

The net CF was highly variable across the 4 studied SHPs, ranging from a sink of −3495.7 ± 767.8 to a source of 735.3 ± 472.2 g $CO_2$e $kWh^{-1}$ (figure 4). However, consistent with the individual system C fluxes, the net CF was largely determined by the operation type of each SHP (storage vs. non-storage). Specifically, the net CF was higher (in absolute terms) in the two SHPs with storage facilities, while it was close to the equilibrium (net CF balance = 0 g $CO_2$e $kWh^{-1}$) in the two non-storage SHPs.

The partition of the different CF components also varied significantly among the four individual SHPs but also between operation types (figure 4). In the two SHPs with storage unit, the biogenic components associated to the flooding of the river system contributed to most of the resulting CF in absolute terms. Specifically, the burial component for SHP 3 (−5144.6 ± 757.6 g $CO_2$e $kWh^{-1}$) and the surface emission component for SHP 4 (709.9 ± 470.5 g $CO_2$e $kWh^{-1}$) dominated their respective CFs. Conversely, in the two non-storage plants, the non-biogenic flux components associated with the construction and operation of the SHPs, as well as the turbine-derived flux contributed together to most of the resulting CF. In this case, the partitioning of these three components was similar between SHPs. The construction, operation and turbine CF component were within the same order of magnitude in the four 4 SHPS regardless of their size and operation type. Results of the error propagation for the net CF for each SHP in table S5.

### 3.4. Storage capacity and CF of small hydropower

The water residence time of two non-storage SHPs was much lower (few hours) than that of the two storage plants (>55 d in both cases, table S3). The magnitude of the gross non-biogenic CF for the studied SHPs was low (8.0–17.1 g $CO_2$e $kWh^{-1}$) and did not change significantly with increases in the

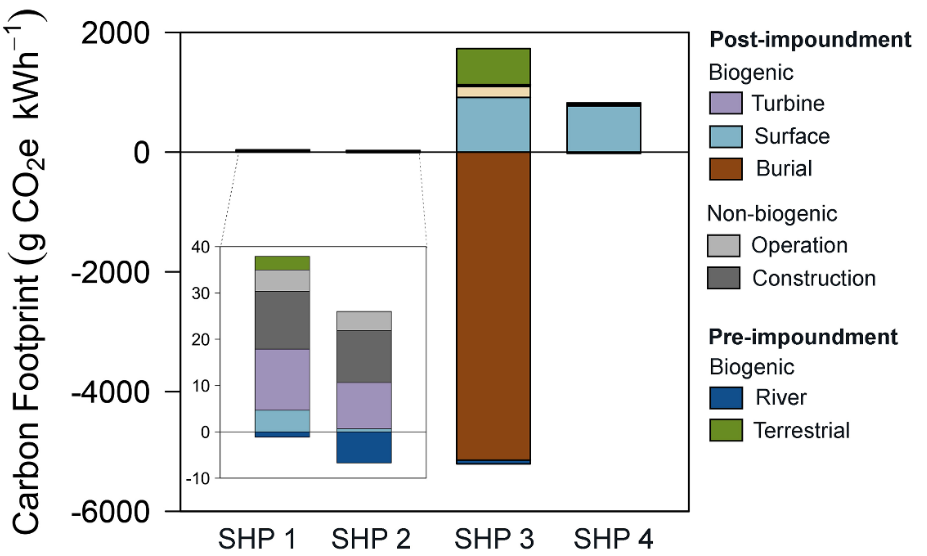


**Figure 4.** Net carbon footprint (CF) of the four SHPs over a 100 years life cycle, and partitioned by flux component (scheme and description of flux components considered in the CF assessment in figure S2 and table S1). Note that the $y$-axis scale range of the two non-storage SHPs (SHP 1 and SHP 2) is lower than the scale of the main panel.

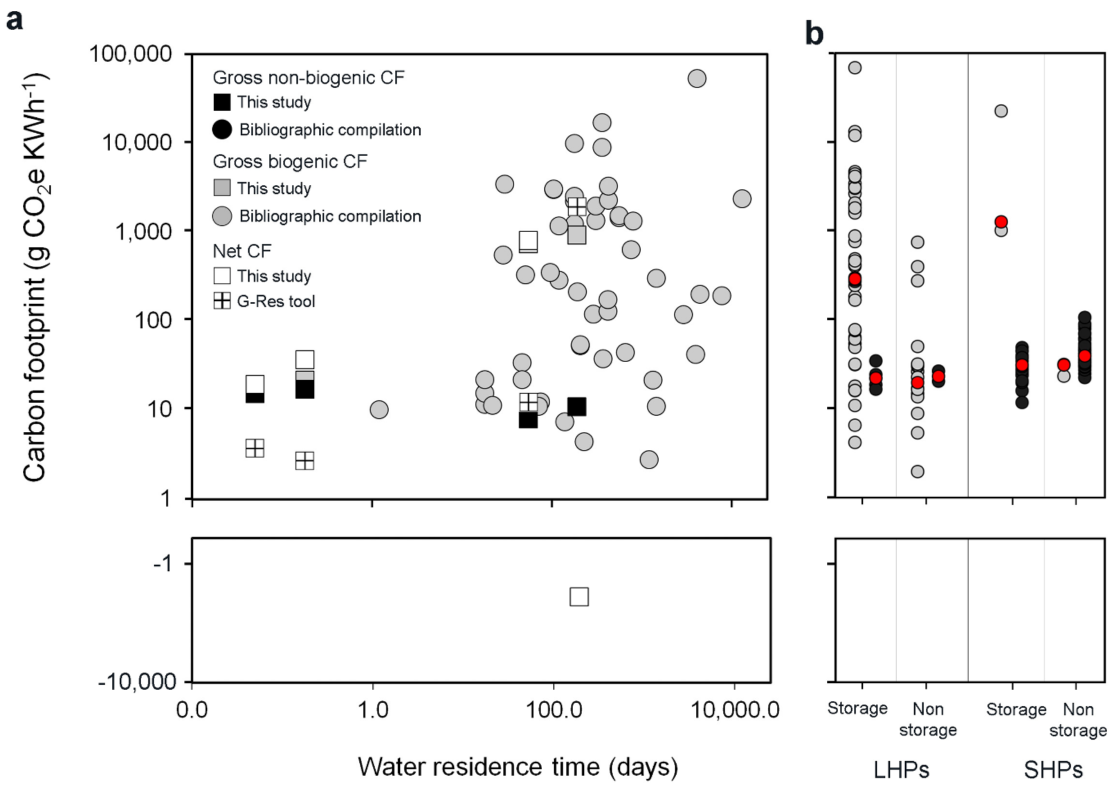


**Figure 5.** (a) Gross and net carbon footprint (CF) of HPs across a reservoir water residence time gradient. Squares represent HPs assessed in this study. Circles represent bibliographic data from Hertwich *et al* (2013) ($n = 73$). Grey and black color represents gross CF estimates (i.e. only accounting for post-impoundment conditions) considering respectively biogenic and non-biogenic carbon flux components (figure S2 and table S1 for definitions). White color represents the net CF (i.e. accounting for both post- and pre-impoundment conditions) for the studied SHPs components (figure S2). White squares with a cross represent the net CF for the studied sites computed with the web-based GHG reservoir (G-res) tool developed by the UNESCO/IHA to unify global hydropower CFs assessments. (b) Aggregation of individual HPs CF by installed power capacity (LHPs are HPs with installed power >10 MW; SHPs are HPs with power capacity lower than 10 MW) and operation type (non-storage and storage). Red circles represent medians for the different levels.

water residence time or with changes in operation types (black squares in figure 5(a)). In contrast, the gross biogenic CF for the studied SHPs was clearly related to the water residence time, a pattern that remained consistent over the larger range of sizes reported in the literature (grey squares in figure 5(a)). Based on this distribution, the magnitude of gross CF observations tended to be lower and stable until a threshold of ca. 25 d (figure 5(a)). From this value on, the dispersion of the CF dataset increased abruptly, and the observations covered indistinctly all the CF range. As an example, some of the HPs reached values close to the equilibrium (net CF = 0 g $CO_2$e $kWh^{-1}$) or even negative, in those situations when the burial and pre-impoundment C fluxes were incorporated into the CF (see figure 4).

To explore whether, reservoir hydrodynamics associated with operation type was the most determining factor on driving the CF, we categorized the dataset of literature values by operation type (non-storage and storage) and by installed power capacity, differentiating SHPs (<10 MW) from large HPs (LHP, >10 MW). The highest and more variable CFs (figure 5(b)) were associated to the plants with storage facilities, irrespective of the installed capacity (LHPs vs. SHPs) The median gross CF for large and small storage HPs was respectively 206.2 and 924.8 g $CO_2$e $kWh^{-1}$ (interquartile range = 1477.1 and 8164.6, respectively). In contrast, the median CF for large and small non-storage HPs was respectively 13.5 and 18.9 g $CO_2$e $kWh^{-1}$ (interquartile range = 14.95 and 2.9 respectively).

## 4. Discussion

We applied a LCA to quantify, partition, and compare the net CF of four temperate SHPs with different operation designs over a 100 year time horizon. In contrast with previous hydropower LCAs studies, here we accounted for all potential sources and sinks of C within the life cycle of the studied SHPs, including both biogenic and non-biogenic sources, as well as for the pre- and post-impoundment stages involved in the flooding of a reservoir. Irrespective of the power installed in the SHPs, the areal and system-level C emissions were mostly driven by the residence time of the impoundment water, which is, in turn, linked to the SHP operation type. Accordingly, non-storage SHPs were almost neutral in terms of the CF, while SHPs with storage facilities prolonged the water residence time in the reservoir and either acted as a source or sink of C. Storage facilities promoted either emission of biogenic gases, mostly methane, from the surface or C storage in the sediments. Our work shows that integrative net CF examination accounting for different operation designs is necessary to better comprehend the environmental impacts of SHPs.

### 4.1. The relevance of storage capacity for the CF of SHPs

Dam size (e.g. height, width) influences many river ecosystem processes, among them the likelihood of temperature stratification or the dam's effectiveness as a barrier to fish migration and sediment transport (Poff and Hart 2002). Dam size also interacts with dam operations and river hydrology to influence key hydraulic variables (e.g. water residence time, the area and the volume of the reservoir, or its ability to buffer peak flows), which in turn affect many different facets of the biophysical regime (Poff and Hart 2002, Maavara *et al* 2020). Here we show that the magnitude of the CFs in SHPs is also controlled by the capacity of the SHP to store water (addressed as water residence time), which is closely connected to the likelihood of biogenic processes associated with the impoundment of the river and the flooding of the terrestrial systems to be more or less active (Battin *et al* 2008). Although defined as small hydropower according to current classification criteria (Couto and Olden 2018), our SHPs with storage reservoirs (SHP 3 and SHP 4) promoted processes typically associated to lentic water bodies with long water residence times, such as decomposition and sedimentation of the organic matter (Catalán *et al* 2016, Mendonça *et al* 2017). In contrast, the hydrologic behavior of SHP 1 and SHP 2 was more similar to that of running waters reaches with shallow depths and water residence times of few hours. These conditions do not promote the development of anaerobic respiratory processes, resulting in almost undetectable areal rates of $CH_4$, the flux that has the highest contribution to the CFs of the two SHPs with larger water storage capacity (Gómez-Gener *et al* 2018).

Our study also identifies biogenic C emissions from the water surface of the two storage SHPs as one of the major C fluxes contributing to their CFs. The contribution of $CH_4$ emissions to the CF was comparable to, or greater than that of $CO_2$, even when not converted to $CO_2$e units. This observation is expected in systems with significant accumulation of organic matter due to water impoundment (Maeck *et al* 2013). Actually, the areal $CH_4$ emission rates measured in the storage SHPs are comparable to those reported from tropical reservoirs (St Louis *et al* 2000, Barros *et al* 2011, Deemer *et al* 2016), suggesting that mid-latitude temperate reservoirs can also emit large amounts of $CH_4$. The main pathway of surface $CH_4$ emissions for the two storage systems was ebullition. High rates of ebullitive $CH_4$ emissions were commonly paired with high rates of diffusion, possibly due to dissolution of the $CH_4$ bubbles throughout their transit from the sediment to the water surface (DelSontro *et al* 2010). Actually the areal ebullition rates reported for SHP 4 were around the highest ever measured from reservoir surfaces (up to 3180 mmol $CH_4$ $m^{-2}$ $d^{-1}$; (Deemer *et al* 2016). In contrast, $CH_4$ emissions from the surface of the two non-storage SHPs was very low and dominated by diffusion, an observation that exemplifies the rather riverine behavior of these two SHPS (Deemer *et al* 2016).

Another CF component that is clearly associated to the storage capacity of the SHPs is the C burial flux, which in the case of SHP 3 was critical to define the SHP as a net $CO_2$e sink. In this particular SHP, the measured areal sedimentation rate (31.7 g $CO_2e$ $m^{-2}$ $d^{-1}$; figure 3) was extremely high and clearly falls in the upper range for reservoirs (Mendonça *et al* 2017) and even for small hyperproductive lakes draining agricultural catchments (Downing *et al* 2008). Flooded reservoir sediments can constitute relevant organic C sinks, in which mineralization of large inputs of allochthonous and autochthonous organic matter is often limited by low exposure to oxygen in the sediments (Sobek *et al* 2009).

Other relevant parameters associated to dam size and water storage capacity are total surface area and C emissions from the reservoir drawdown areas. Drawdown areas are the margins of reservoirs that experience water level fluctuations due to seasonal hydrological cycles (e.g. droughts) or dam operation (Kosten *et al* 2018, Marcé *et al* 2019). Therefore, C fluxes associated to these areas are only relevant at the storage SHPs, where water level oscillations allow the exposure of emerged sediment belts. In this study, we measured high $CO_2$ emission rates from the drawdown areas of the two storage SHPs. In one of the systems (SHP 3), these emissions accounted for up to 10% of the total emissions Sediment exposure to air promotes the aerobic respiration of organic matter, releasing a fraction of the buried organic carbon as $CO_2$ to the atmosphere. Conversely, emissions of $CH_4$ were negligible in these areas, probably due to high oxygenation of the sediments and associated constraint for anaerobic processes to occur (Koschorreck and Darwich 2003). Although traditionally ignored, our results indicate that accounting for C emissions (specially $CO_2$) from drawdown areas is needed not only to leverage the role of reservoirs in the global carbon cycle (Keller *et al* 2021) but also to better constrain hydropower CFs.

### 4.2. Gross versus net life-cycle assessments to unravel the CF of SHP

Available quantifications of CFs for hydroelectric energy production are highly variable (Hertwich 2013; figure 5), including values from 0.3 (Raadal *et al* 2011), to values close to 53 295 $gCO_2e$ $kWh^{-1}$ in tropical reservoirs (de Faria *et al* 2015, Almeida *et al* 2019a). For small hydroelectric energy production, results are a bit more constrained but still highly variable, ranging from 8 to 17 071 $gCO_2e$ $kWh^{-1}$ (Hertwich 2013). Although the size-range and the methodologies used for theses estimations are diverse, to the best of our knowledge, no previous study has reported a negative CF, such as the one observed in SHP 3. CFs based on gross fluxes estimations have been obtained across climatic conditions, pre-impoundment land cover types and hydropower technologies (Kumar *et al* 2011, Hertwich 2013, Scherer and Pfister 2016). However, only a limited number of studies considers the net emissions from hydropower (i.e. incorporating all present biogenic and non-biogenic emissions and pre-existing natural emissions). The extreme case represented by SHP 3 (with an absolute difference between gross and net CF of 4403 $gCO_2e$ $kWh^{-1}$, figure 5) highlights the importance of estimating the CF of storage hydroelectric plants through a net balance that integrates all present and past C fluxes (Prairie *et al* 2018, Levasseur *et al* 2021).

Aiming at unifying global hydropower CFs assessments to set more solid foundations for future decisions related to HP production and its climate impact, the International Hydropower Association (IHA) and UNESCO have developed the web-based GHG reservoir (G-res) tool (Prairie *et al* 2017, Harrison *et al* 2021). Here we used the G-res tool to compute the CF for our four study SHPs and compared the results with our own estimates (figure 5(a)). While modeled results based on the G-res tool are valid to predict the CFs of SHPs with shorter water residence times (SHP 1 and 2), results from this comparison showed a poor fit between approaches for our SHPs with water storage capability (SHP 3 and 4). The G-res assessment framework uses a methodology based on empirical measurements from more than 200 reservoirs worldwide. However, studies on SHPs are underrepresented with respect to large HPs. We suggest including a broader range of HP sizes and typologies in the empirical relationships driving G-res tool calculations in future updates of the tool.

### 4.3. Implications for GHG mitigation

The large-scale proliferation of SHPs (Zarfl *et al* 2015, Belletti *et al* 2020, Zarfl and Lehner 2020) has come along with efforts to improve the operation and power generation capacities, to adapt to new social and environmental requirements, and to develop more robust and cost-effective technological solutions (Kumar *et al* IPCC). Recent studies have also focused on the ecological impacts of damming to develop tools aiming at balancing the benefits of hydropower production with maintaining ecosystem services and biodiversity conservation (Couto and Olden 2018, Lange *et al* 2018). However, there are still important knowledge gaps. For instance, there is no consensus on the use of small hydropower as an energy source compatible with climate change mitigation strategies (Kumar *et al* 2011). When assessed in relation to the power generation capacity (installed capacity) per unit of reservoir flooded area, the so-called power density, the environmental footprint becomes a key criterion for sustainable energy planning (www.iea.org/). In relative terms, projects with low GHG emission (e.g. oligotrophic reservoirs) can still have high CFs if they produce low amounts of electricity per unit flooded area (i.e. low power density). Projects with power densities above 4 MW $km^{-2}$ are actually considered climate-friendly and thus eligible for funding by the Clean Development Mechanism f (https://cdm.unfccc.int).

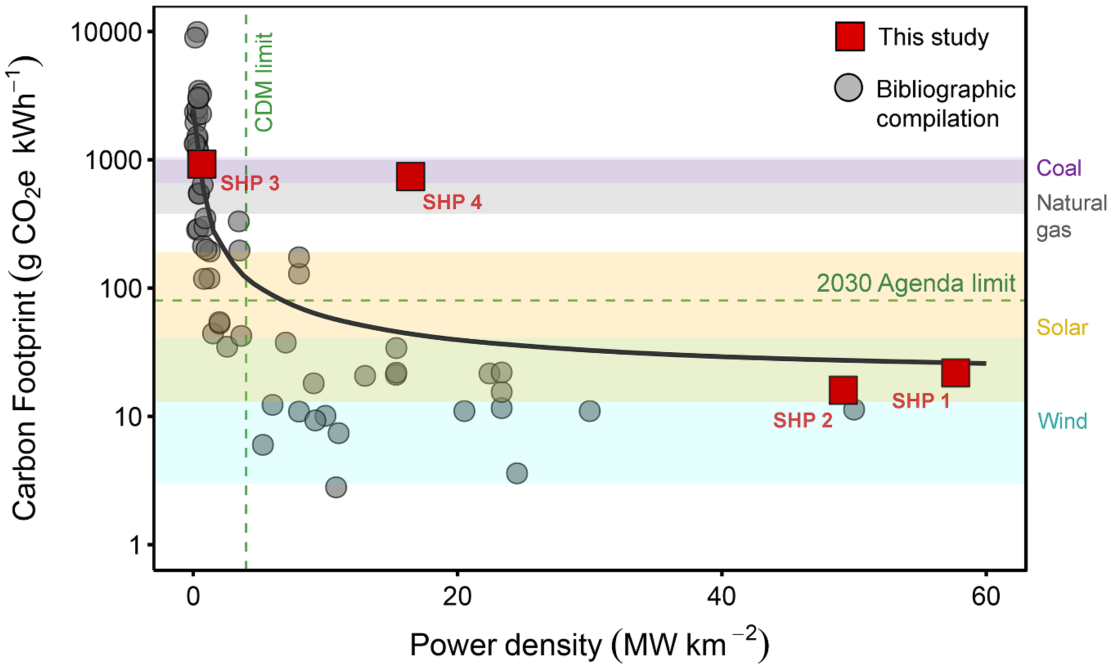


**Figure 6.** Relationship between the power density and the carbon footprint (CF) of HPs from our study (red squares) and from a bibliographic compilation (grey circles, Hertwich 2013, $n = 73$; model line, Almeida *et al* 2019b, $n = 464$). For comparative purposes, results correspond to the 'gross biogenic' CF (see figure S2(a)). Observations that fall both below and to the right of the green dashed lines are plants with CF to power density ratios that satisfy sustainable electricity production goals over a period of 100 years (CFs <80 g $CO_2$e $KWh^{-1}$, International Energy Agency; power density 4 MW $km^{-2}$, Clean Development Mechanism, CDM). The ranges of carbon intensities of coal, natural gas, solar and wind power plants reported by the IPCC are shown in the purple, grey, yellow and green bands, respectively (Kumar *et al* 2011), and used here as a reference.

To frame the domain in which sustainable energy goals are satisfied (i.e. <80 g $CO_2$eq $KWh^{-1}$ and power densities >4 MW $km^{-2}$), we plotted the relationship between power density and C footprint from a compilation of HPs (figure 6). Only around half of the HPs fall within the domain of sustainable electricity production, an observation that is consistent with results from Hertwich (2013) and Almeida *et al* (2019b). In our study, two of the four SHPs (SHP 1 and SHP 2) satisfy sustainable energy goals (figure 6) and result in CFs that are comparable to those from renewable power sources such as solar (photovoltaic) or wind. In contrast, SHP 3 and SHP 4 fall in the highest range of CFs, comparable to those from coal and natural gas thermal plants. Given the current boom in SHPs construction worldwide, proper planning is crucial. Our analysis suggests that prioritizing projects with high power densities, more specifically non-storage SHPs that have been shown to have the lowest generation and emission of GHGs, can attenuate CFs of future hydropower dam portfolios. However we want to stress that the sustainability assessment discussed here was strictly based on CFs considerations. Clearly, decisions to build or remove HPs must involve a more diverse set of factors including social, environmental and cultural aspects (e.g. river ecology, deforestation, loss of biodiversity, human migrations). But to properly balance the social benefits of hydropower against the social and environmental costs of damming up rivers we need to develop more robust and reproducible methodologies that overcome the challenges associated with hydropower CFs assessments. One of the main challenges is the uncertainty associated with the flux estimations for different biogenic and non-biogenic components. For example, the emissions of GHGs from reservoirs can be highly variable in space, and this depends on factors such as temperature, water depth, or catchment land cover. In addition, reservoir are complex ecosystems that operate over long time periods. Consequently, the environmental impacts associated with hydropower are highly variable over time due to factors such as changing climate conditions, water flow rates, and sedimentation rates. Despite these challenges, the LCA framework can still be a useful tool for assessing the environmental impacts of hydropower, when the temporal variability of these impacts is properly accounted for. For example, capturing the dynamics of the system over time might involve using new sensing or satellite technologies to derive time-series of GHGs or remote sensing based water level or water quality parameter (e.g. sedimentation rates).

## Data availability statement

All data that support the findings of this study are included within the article (and any supplementary files).

## Acknowledgments

This study was supported by projects PID2020-114024GB-C31 and PID2020-114024GB-C32, funded by MCIN/AEI/10.13039/501100011033/, and by a Research Grant on Energy and Environment funded by Fundación Iberdrola España. L G was further supported by a fellowship from "la Caixa" Foundation (ID 100010434) and from the European Union's Horizon 2020 research and innovation programme under the Marie Skłodowska Curie Grant Agreement No. 847648 (fellowship: LCF/BQ/PI21/11830034). The funders of the study had no role in study design, data collection, data analysis, data interpretation, or writing of this manuscript. We acknowledge logistic support by Aguas del Añarbe and Arturo Elosegi during fieldwork. The author's have confirmed that any identifiable participants in this study have given their consent for publication.

## ORCID iDs

Lluís Gómez-Gener https://orcid.org/0000-0003-3279-3589
Daniel von Schiller https://orcid.org/0000-0002-9493-3244
Rafael Marcé https://orcid.org/0000-0002-7416-4652
Biel Obrador https://orcid.org/0000-0003-4050-0491

## References

Almeida R M *et al* 2019b Reducing greenhouse gas emissions of Amazon hydropower with strategic dam planning *Nat. Commun.* **10** 4281

Almeida R M, Paranaíba J R, Barbosa Í, Sobek S, Kosten S, Linkhorst A, Mendonça R, Quadra G, Roland F and Barros N 2019a Carbon dioxide emission from drawdown areas of a Brazilian reservoir is linked to surrounding land cover *Aquat. Sci.* **81** 68

Anderson D, Moggridge H, Warren P and Shucksmith J 2015 The impacts of 'run-of-river' hydropower on the physical and ecological condition of rivers *Water Environ. J.* **29** 268–76

Barros N, Cole J J, Tranvik L J, Prairie Y T, Bastviken D, Huszar V L M, del Giorgio P and Roland F 2011 Carbon emission from hydroelectric reservoirs linked to reservoir age and latitude *Nat. Geosci.* **4** 593–6

Battin T J, Kaplan L A, Findlay S, Hopkinson C S, Marti E, Packman A I, Newbold J D and Sabater F 2008 Biophysical controls on organic carbon fluxes in fluvial networks *Nat. Geosci.* **1** 95–100

Beaulieu J, McManus M and Nietch C 2016 Estimates of reservoir methane emissions based on a spatially-balanced probabilistic-survey *Limnol. Oceanogr.* **61** S27–40

Belletti B *et al* 2020 More than one million barriers fragment Europe's rivers *Nature* **588** 436–41

Bertassoli D J, Sawakuchi H O, de Araújo K R, de Camargo M G P, Alem V A T, Pereira T S, Krusche A V, Bastviken D, Richey J E and Sawakuchi A O 2021 How green can Amazon hydropower be? Net carbon emission from the largest hydropower plant in Amazonia *Sci. Adv.* **7** eabe1470

Catalán N, Marcé R, Kothawala D N and Tranvik Lars J 2016 Organic carbon decomposition rates controlled by water retention time across inland waters *Nat. Geosci.* **9** 501–4

Couto T B A and Olden J D 2018 Global proliferation of small hydropower plants *Front. Ecol. Environ.* **16** 91–100

de Faria F A, Jaramillo P, Sawakuchi E, Richey J E and Barros N 2015 Estimating greenhouse gas emissions from future Amazonian hydroelectric reservoirs *Environ. Res. Lett.* **14** 124019

Deemer B R, Harrison J A, Li S, Beaulieu J J, DelSontro T, Barros N, Bezerra-Neto J F, Powers S M, Dos Santos M A and Vonk J A 2016 Greenhouse gas emissions from reservoir water surfaces: a new global synthesis *BioScience* **66** 949–64

DelSontro T, McGinnis D F, Sobek S, Ostrovsky I and Wehrli B 2010 Extreme methane emissions from a Swiss hydropower reservoir: contribution from bubbling sediments *Environ. Sci. Technol.* **44** 2419–25

Downing J A *et al* 2006 The global abundance and size distribution of lakes, ponds, and impoundments *Limnol. Oceanogr.* **51**

Downing J A, Cole J J, Middelburg J J, Striegl R G, Duarte C M, Kortelainen P, Prairie Y T and Laube K A 2008 Sediment organic carbon burial in agriculturally eutrophic impoundments over the last century: sediment organic carbon burial *Glob. Biogeochem. Cycles* **22** GB1018

Edenhofer O, Pichs-Madruga R, Sokona Y, Seyboth K, Matschoss P, Kadner S and von Stechow C 2011 *Renewable Energy Sources and Climate Change Mitigation* (Cambridge University Press) (https://doi.org/10.1017/CBO9781139151153)

Friedlingstein P *et al* 2019 Global carbon budget 2019 *Earth Syst. Sci. Data* **11** 1783–838

Gómez-Gener L, Gubau M, von Schiller D, Marcé R and Obrador B 2018 Effect of small water retention structures on diffusive $CO_2$ and $CH_4$ emissions along a highly impounded river *Inland Waters* **8** 449–60

Guérin F, Abril G, Richard S, Burban B, Reynouard C, Seyler P and Delmas R 2006 Methane and carbon dioxide emissions from tropical reservoirs: significance of downstream rivers *Geophys. Res. Lett.* **33** L21407

Harrison J A, Prairie Y T, Mercier-Blais S and Soued C 2021 Year-2020 global distribution and pathways of reservoir methane and carbon dioxide emissions according to the greenhouse gas from reservoirs (G-res) model *Glob. Biogeochem. Cycles* **35** e2020GB006888

Hertwich E G 2013 Addressing biogenic greenhouse gas emissions from hydropower in LCA *Environ. Sci. Technol.* **47** 9604–11

Keller P S, Marcé R, Obrador B and Koschorreck M 2021 Global carbon budget of reservoirs is overturned by the quantification of drawdown areas *Nat. Geosci.* **14** 402–8

Kelly-Richards S, Silber-Coats N, Crootof A, Tecklin D and Bauer C 2017 Governing the transition to renewable energy: a review of impacts and policy issues in the small hydropower boom *Energy Policy* **101** 251–64

Kibler K M and Tullos D D 2013 Cumulative biophysical impact of small and large hydropower development in Nu River, China: biophysical impact of small and large hydropower *Water Resour. Res.* **49** 3104–18

Koschorreck M and Darwich A 2003 Nitrogen dynamics in seasonally flooded soils in the Amazon floodplain *Wetl. Ecol. Manage.* **11** 317–30

Kosten S, van den Berg S, Mendonça R, Paranaíba J R, Roland F, Sobek S, van den Hoek J and Barros N 2018 Extreme drought boosts $CO_2$ and $CH_4$ emissions from reservoir drawdown areas *Inland Waters* **8** 329–40

Kumar A, Schei T, Ahenkorah A, Rodriguez R C, Devernay J M, Freitas M, Hall D, Killingtveit Å and Liu Z 2011 Hydropower *IPCC Special Report on Renewable Energy Sources and Climate Change Mitigation* ed O Edenhofer *et al* (Cambridge University Press) pp 437–96

Lange K, Meier P, Trautwein C, Schmid M, Robinson C T, Weber C and Brodersen J 2018 Basin-scale effects of small

hydropower on biodiversity dynamics *Front. Ecol. Environ.* **16** 397–404
Lehner B *et al* 2011 High-resolution mapping of the world's reservoirs and dams for sustainable river-flow management *Front. Ecol. Environ.* **9** 494–502
Levasseur A, Mercier-Blais S, Prairie Y T, Tremblay A and Turpin C 2021 Improving the accuracy of electricity carbon footprint: estimation of hydroelectric reservoir greenhouse gas emissions *Renew. Sustain. Energy Rev.* **136** 110433
Maavara T, Chen Q, van Meter K, Brown L E, Zhang J, Ni J and Zarfl C 2020 River dam impacts on biogeochemical cycling *Nat. Rev. Earth Environ.* **1** 103–16
Maeck A, Delsontro T, McGinnis D F, Fischer H, Flury S, Schmidt M, Fietzek P and Lorke A 2013 Sediment trapping by dams creates methane emission hot spots *Environ. Sci. Technol.* **47** 8130–7
Marcé R, Obrador B, Gómez-Gener L, Catalán N, Koschorreck M, Arce M I, Singer G and von Schiller D 2019 Emissions from dry inland waters are a blind spot in the global carbon cycle *Earth Sci. Rev.* **188** 240–8
McGinnis D F, Greinert J, Artemov Y, Beaubien S E and Wüest A 2006 Fate of rising methane bubbles in stratified waters: how much methane reaches the atmosphere? *J. Geophys. Res.* **111** C09007
Mendonca R, Kosten S, Sobek S, Jaqueline Cardoso S, Paulo Figueiredo-Barros M, Estrada C H D and Roland F 2016 Organic carbon burial efficiency in a subtropical hydroelectric reservoir *Biogeosciences* **13** 3331–42
Mendonça R, Müller R A, Clow D, Verpoorter C, Raymond P, Tranvik L J and Sobek S 2017 Organic carbon burial in global lakes and reservoirs *Nat. Commun.* **8** 1694
Pacca S 2007 Impacts from decommissioning of hydroelectric dams: a life cycle perspective *Clim. Change* **84** 281–94
Palmer M and Ruhi A 2019 Linkages between flow regime, biota, and ecosystem processes: implications for river restoration *Science* **365** eaaw2087
Pang M, Zhang L, Wang C and Liu G 2015 Environmental life cycle assessment of a small hydropower plant in China *Int. J. Life Cycle Assess* **20** 796–806
Paranaíba J R *et al* 2022 Cross-continental importance of $CH_4$ emissions from dry inland-waters *Sci. Total Environ.* **814** 151925
Poff N L and Hart D D 2002 How dams vary and why it matters for the emerging science of dam removal *BioScience* **52** 659
Prairie Y T *et al* 2018 Greenhouse gas emissions from freshwater reservoirs: what does the atmosphere see? *Ecosystems* **21** 1058–71
Prairie Y T, Alm J, Harby A, Mercier-Blais S and Nahas R 2017 Technical documentation, UNESCO/IHA research project on the GHG status of freshwater reservoirs version 1.1
Prairie Y T, Mercier-Blais S, Harrison J A, Soued C, del Giorgio P, Harby A, Alm J, Chanudet V and Nahas R 2021 A new modelling framework to assess biogenic GHG emissions from reservoirs: the G-res tool *Environ. Model. Softw.* **143** 105117
Raadal H L, Gagnon L, Modahl I S and Hanssen O J 2011 Life cycle greenhouse gas (GHG) emissions from the generation of wind and hydro power *Renew. Sustain. Energy Rev.* **15** 3417–22
Räsänen T A, Varis O, Scherer L and Kummu M 2018 Greenhouse gas emissions of hydropower in the Mekong River Basin *Environ. Res. Lett.* **13** 034030
Rosentreter J A *et al* 2021 Half of global methane emissions come from highly variable aquatic ecosystem sources *Nat. Geosci.* **14** 225–30
Scherer L and Pfister S 2016 Hydropower's biogenic carbon footprint *PLoS One* **11** e0161947
Serça D *et al* 2016 Nam Theun 2 Reservoir four years after commissioning: significance of drawdown methane emissions and other pathways *Hydroecologie Appl.* **19** 119–46
Sobek S, Durisch-Kaiser E, Zurbrügg R, Wongfun N, Wessels M, Pasche N and Wehrli B 2009 Organic carbon burial efficiency in lake sediments controlled by oxygen exposure time and sediment source *Limnol. Oceanogr.* **54** 2243–54
Soued C, Harrison J A, Mercier-Blais S and Prairie Y T 2022 Reservoir $CO_2$ and $CH_4$ emissions and their climate impact over the period 1900–2060 *Nat. Geosci.* **15** 700–5
St Louis V L, Kelly C A, Duchemin É, Rudd J W M and Rosenberg D M 2000 Reservoir surfaces as sources of greenhouse gases to the atmosphere: a global estimate *BioScience* **50** 766
Turconi R, Boldrin A and Astrup T 2013 Life cycle assessment (LCA) of electricity generation technologies: overview, comparability and limitations *Renew. Sustain. Energy Rev.* **28** 555–65
Varun, Bhat I K and Prakash R 2009 LCA of renewable energy for electricity generation systems-A *Renew. Sustain. Energy Rev.* **13** 1067–73
Varun, Prakash R and Bhat I K 2012 Life cycle greenhouse gas emissions estimation for small hydropower schemes in India *Energy* **44** 498–508
Weisser D 2007 A guide to life-cycle greenhouse gas (GHG) emissions from electric supply technologies *Energy* **32** 1543–59
WSHPDR 2019 *WSHPDR (World Small Hydropower Development Report 2019)* (Vienna)
Yang M, Geng X, Grace J, Lu C, Zhu Y, Zhou Y and Lei G 2014 Spatial and seasonal $CH_4$ flux in the littoral zone of Miyun Reservoir near Beijing: the effects of water level and its fluctuation *PLoS One* **9** e94275
Zarfl C and Lehner B 2020 Small barriers are a big deal for Europe's rivers *Nature* **588** 395–6
Zarfl C, Lumsdon A E, Berlekamp J, Tydecks L and Tockner K 2015 A global boom in hydropower dam construction *Aquat. Sci.* **77** 161–70
Zhang Q, Karney B, MacLean H L and Feng J 2007 Life-cycle inventory of energy use and greenhouse gas emissions for two hydropower projects in China *J. Infrastruct. Syst.* **13** 271–9